Journal of Chromatography, 646 (1993) 3–15
Elsevier Science Publishers B.V., Amsterdam

CHROMSYMP. 2863

Experimental and theoretical studies of rate constant evaluation by affinity chromatography

Determination of rate constants for the interaction of saccharides with concanavalin A

Peter D. Munro and Donald J. Winzor*

Department of Biochemistry, University of Queensland, Brisbane, Queensland 4072 (Australia)

John R. Cann

Department of Biochemistry/Biophysics/Genetics and the University of Colorado Cancer Center, University of Colorado Health Sciences Center, Denver, CO 80262 (USA)

ABSTRACT

Experimental studies have been combined with numerical simulations of frontal affinity chromatography to illustrate the potential of this technique for obtaining rate constants for the interaction of the solute with affinity matrix and for a reaction in competition with the solute–matrix interaction. Frontal chromatography of *p*-nitrophenylmannoside on a standard HPLC column of concanavalin A–CPG 3000 at flow-rates of 2–10 ml/min has yielded a rate constant of 0.42 s^{-1} for the dissociation of the solute-immobilized lectin complex on the basis of the flow-rate dependence of boundary spreading in the elution profile: this constant (k_{-1}) has been obtained by extrapolating the apparent dissociation rate constant (k_{-1}^{obs}) to zero solute concentration to eliminate the consequences of non-linear (Langmuir) kinetics. Numerical simulations of the affinity chromatographic behaviour of *p*-nitrophenylmannoside (A) in the presence of a fixed concentration of a second saccharide (B) that competes for matrix sites have shown that the corresponding extrapolation of k_{-1}^{obs} to zero solute concentration again yields k_{-1}, but that the presence of competing saccharide is manifested as a change in slope of the essentially linear dependence of k_{-1}^{obs} upon *p*-nitrophenylmannoside concentration ([A]). A calibration plot of the variation of $d(k_{-1}^{obs})/d[A]$ with dissociation rate constant for the competing ligand–matrix interaction (k_{-2}) has then been used to obtain a rate constant of 1 s^{-1} for the dissociation of methylmannoside from the immobilized lectin on the basis of frontal affinity chromatography of *p*-nitrophenylmannoside in the presence of 100 μM competing saccharide. Finally, the potential of affinity chromatography for evaluating the dissociation rate constant for a competing interaction between ligand and solute has been illustrated by numerical simulation of elution profiles and their interpretation in terms of a published expression for the flow-rate dependence of boundary spreading under conditions of linear kinetics; and by extrapolation of the apparent rate constants so obtained to zero solute concentration to take into account the effects of Langmuir kinetics on chromatographic migration.

INTRODUCTION

Studies of the kinetics of ligand binding have generally been confined to interactions for which the rate of reaction is either sufficiently fast for study by stopped-flow and temperature-jump techniques, or sufficiently slow for study by the classical procedure of analyzing product formation after reaction for a series of time intervals. Unfortunately, the time scale of metabolic flux is such that kinetic considerations are likely to be

* Corresponding author.

0021-9673/93/$06.00

of greatest importance for reactions in the intervening range, which has been largely neglected for want of suitable methodology.

In principle, high-performance liquid affinity chromatography has the potential to provide a means of determining rate constants that are too slow for study by stopped-flow techniques [1–6]. Furthermore, despite the failure of those initial investigations to provide much encouragement for the experimental realization of that potential, a more recent study [7] has demonstrated the experimental feasibility of employing affinity chromatography to characterize the kinetics of the solute–matrix interaction. The present extension of that investigation is concerned with kinetic characterization of a reaction in competition with the solute–matrix interaction.

The initial aim of this investigation is to verify the envisaged experimental approach by numerical simulations of the chromatographic migration of *p*-nitrophenylmannoside (solute) on immobilized concanavalin A, a system for which literature estimates of the required rate and equilibrium constants are available [4,5,8,9]. Two competitive situations are considered: (i) ligand-facilitated elution of solute arising from supplementation of the applied solution with a second saccharide that competes for concanavalin A sites on the affinity matrix; and (ii) ligand-facilitated elution of solute arising from supplementation of the applied solution with concanavalin A to decrease the concentration of *p*-nitrophenylmannoside available for interaction with affinity matrix. The experimental aspects of the procedure are illustrated by means of a frontal chromatographic study of the effect of methylmannoside on the elution of *p*-nitrophenylmannoside from concanavalin A immobilized on CPG-3000 under conditions of Langmuir (non-linear) kinetics.

EXPERIMENTAL

Materials

Concanavalin A, controlled-pore glass beads (glyceryl-CPG 3000, 200 mesh), *p*-nitrophenyl α-D-mannoside, and methyl α-D-mannoside were obtained from Sigma (St. Louis, MO, USA). The tresylation procedure described by Nilsson and Larsson [3] was used to immobilize concanavalin A on the glyceryl-CPG 3000 beads. Because the effective thermodynamic concentration of immobilized ligand sites is the relevant column parameter for quantitative affinity chromatography, the lectin content of the affinity column has been defined on that basis rather than analytically.

Affinity chromatography of saccharides on immobilized concanavalin A

The interaction of *p*-nitrophenylmannoside with immobilized concanavalin A was quantified by subjecting solutions of the saccharide (10.7–53.4 μM) to frontal chromatography on a column (25 × 0.46 cm) of concanavalin A–CPG 3000 equilibrated at 25°C with phosphate–chloride buffer (0.05 *M* NaH_2PO_4–0.01 *M* Na_2HPO_4–0.001 *M* $MgCl_2$–0.001 *M* $MnCl_2$–0.44 *M* NaCl), pH 5.5. Effluent from the HPLC column, maintained at constant flow-rates in the range 2–10 ml/min by means of a Waters Model 510 pump, was assayed continuously at 305 nm [4] with an ISCO V^4 monitor, the response of which was transferred to an IBM-compatible personal computer by means of a software package designed initially for the evaluation of progress curves in enzyme kinetic studies [10]. The acquired data in the range 3–97% of the plateau concentration for the advancing and trailing elution profiles were analyzed by standard procedures to obtain the first moment (mean elution volume, $\bar{V}_A$) and second moment (σ_A^2) of the boundaries.

For the corresponding characterization of the competitive interaction between methylmannoside and immobilized concanavalin A, the same protocol was followed except that the buffer and applied solutions of *p*-nitrophenylmannoside were supplemented with a fixed concentration (100 μM) of the competing ligand, which did not need to be monitored because of its invariant concentration.

Evaluation of equilibrium constants

Operationally defined values of the association equilibrium constant (K_{AX}) and matrix-site concentration ($[\bar{X}]$) for the interaction of *p*-nitrophenylmannoside (partitioning solute, A) with

matrix sites (X) may be obtained from the expression [11]

$$(\bar{V}_A/V_A^*)^{1/f} - 1 = K_{AX}[\bar{\bar{X}}] - fK_{AX}(\bar{V}_A/V_A^*)^{(f-1)/f} \cdot [A][(\bar{V}_A/V_A^*)^{1/f} - 1] \quad (1a)$$

in which f, the valence of the partitioning solute, is unity for the interaction of *p*-nitrophenylmannoside with immobilized concanavalin A sites. Consequently, eqn. 1a becomes [11–13]

$$(\bar{V}_A/V_A^*) - 1 = K_{AX}[\bar{\bar{X}}] - K_{AX}[A][(\bar{V}_A/V_A^*) - 1] \quad (1b)$$

$\bar{V}_A$ is the measured elution volume in a frontal chromatographic experiment with applied solute concentration [A] on an affinity column with an effective total concentration of matrix sites $[\bar{\bar{X}}]$. V_A^*, the elution volume of solute in the absence of interaction with matrix, was obtained from experiments with *p*-nitrophenylmannoside (10.7 μM) on an identical column of underivatized glyceryl-CPG 3000. As required, the value so obtained coincided with the elution volume of *p*-nitrophenylmannoside in the presence of a sufficiently high concentration (0.2 M) of methylmannoside to effectively eliminate the interaction between immobilized lectin and partitioning solute. For illustrative purposes K_{AX} and $[\bar{\bar{X}}]$ may be obtained as the slope and abscissa intercept, respectively, of a plot of $(\bar{V}_A - V_A^*)/V_A^*$ *versus* [A] $[(\bar{V}_A - V_A^*)/V_A^*]$; but reported values were obtained by non-linear regression analysis in terms of the expression

$$(\bar{V}_A/V_A^*) - 1 = K_{AX}[\bar{\bar{X}}]/(1 + K_{AX}[A]) \quad (1c)$$

of which eqn. 1b is the equivalent of a Scatchard linear transform [11,14].

The quantitative expression describing the elution of *p*-nitrophenylmannoside in frontal experiments conducted with a fixed concentration, [B], of competing saccharide (methylmannoside) is analogous to eqn. 1b except that K_{AX} is replaced by a constitutive equilibrium constant, $\bar{K}_{AX}$, defined [11] by

$$\bar{K}_{AX} = K_{AX}/(1 + K_{BX}[B]) \quad (1d)$$

where K_{BX} is the association equilibrium constant for the competing interaction between B and matrix sites.

Evaluation of kinetic parameters for the solute–matrix interaction

Under conditions of linear kinetics the dependence of the variance (σ_A^2) upon flow-rate, F, in the absence of competing ligand is related to the rate constant for dissociation of A from solute–matrix complex, k_{-1}, by the expression [7,15,16]

$$k_{-1} = 2(\bar{V}_A - V_A^*)/(d\sigma_A^2/dF) \quad (2)$$

where the denominator of the right-hand side is obtained from the linear flow-rate dependence of the second moment of either the advancing or trailing elution profile [7]. Although eqn. 2 does not apply directly to the analysis of results exhibiting Langmuir (non-linear) kinetics, it may be used to define an operational parameter (k_{-1}^{obs}), which may then be extrapolated to infinite dilution ($[A] \rightarrow 0$) to obtain the true dissociation constant [7].

The same experimental approach has been adopted for situations in which the chromatography of partitioning solute (A) is conducted in the presence of a fixed concentration of competing ligand (B). Under these circumstances, however, the value of k_{-1}^{obs} is a combination of rate and equilibrium parameters for solute and competing ligand interactions. The use of these values of k_{-1}^{obs} to evaluate k_{-2}, the rate constant for dissociation of the complex involving competing ligand, is addressed later.

Numerical simulation of elution profiles

For all simulations of elution profiles the column was assigned a diameter of 0.46 cm and a length of 20 cm. Elution profiles were generated by an adaptation of the theoretical plate model of chromatography [17] with the transfer volume set at 10% of the plate (segment) volume accessible to solute. The present simulations follow the procedure described previously [7] for examining the affinity chromatographic behaviour of A alone, which was considered in terms of the reaction

$$A + X \underset{k_{-1}}{\overset{k_{+1}}{\rightleftharpoons}} AX \quad (3a)$$

For simulations of the chromatographic migration of A in the presence of competing ligand, B, the same general procedure has been adopted; but clearly, consideration needs to be given to the consequences of the kinetics of the competing reaction. In addition to considering the present experimental situation in which the completing reaction may be written as

$$B + X \underset{k_{-2}}{\overset{k_{+2}}{\rightleftharpoons}} BX \quad (3b)$$

chromatographic migration has also been simulated for the case where B competes with matrix sites for A: the second reaction then becomes

$$A + B \underset{k_{-3}}{\overset{k_{+3}}{\rightleftharpoons}} AB \quad (3c)$$

In accordance with previous protocol [7], the column matrix was considered to be impervious to solute and competing ligand, a situation which obviates the need to consider the kinetics of solute partitioning into the accessible region of the stationary phase. After each transfer of a volume increment, δV, which corresponds to a time interval (δt) via the flow-rate, F (1–5 ml/min), a subroutine for chemical kinetics was called to evaluate the new distribution of solute(s) between complexed and free states in each column segment (plate). For simulation of the affinity chromatographic migration of A alone this kinetic subroutine [7] entailed analytical solution of the differential rate equation [18]. Simulation of the corresponding behaviour of A in the presence of B required a kinetic subroutine with numerical solution of the set of differential equations by the 4th-order Runge–Kutta method.

RESULTS AND DISCUSSION

Although the major goal of this investigation is the determination of rate constants for the dissociation of saccharide complexes with immobilized concanavalin A, it should be noted that the same experiments also provide a means of evaluating the corresponding association equilibrium constants from the measured elution volumes, $\bar{V}_A$. Unlike the second moment, the elution volume (first moment of the eluted boundary) is independent of flow-rate and is governed by eqn. 1. Estimates of 32.5 μM and 27 000 M^{-1} for [$\bar{X}$] and K_{AX}, respectively, are obtained from the dependence of $\bar{V}_A$ upon concentration of *p*-nitrophenylmannoside, the Scatchard transform of which is illustrated (○) in Fig. 1. Combination of the value of K_{AX} with the value of 14 000 M^{-1} for $\bar{K}_{AX}$ from results obtained in the presence of 100 μM methylmannoside (●) yields, via eqn. 1d, an association equilibrium constant (K_{BX}) of 9 000 M^{-1} for the corresponding interaction between this competing saccharide and immobilized concanavalin A. These association constants are encompassed by the values of 24 000 (±5 000) and 11 000 (±2 000) M^{-1} obtained for K_{AX} and K_{BX}, respectively, in an earlier, more extensive investigation under the same conditions [pH 5.5, ionic

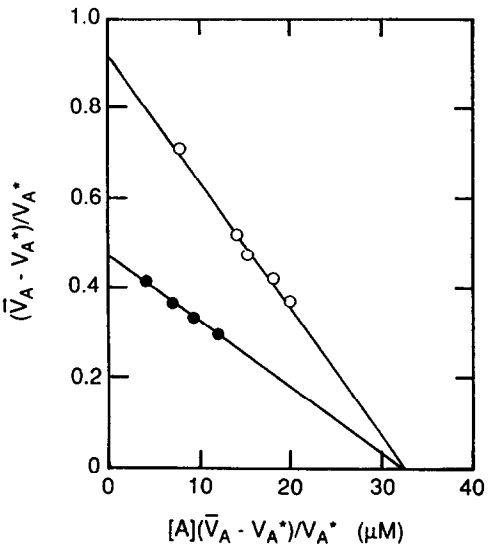

Fig. 1. Scatchard plot for the determination, via eqn. 1b, of the association constant for the solute–matrix interaction (K_{AX}) by frontal affinity chromatography of *p*-nitrophenylmannoside (○) on a glyceryl-CPG 3000 column (25 × 0.46 cm) with concanavalin A as immobilized ligand. The solid symbols refer to evaluation of its constitutive counterpart ($\bar{K}_{AX}$) in the presence of 100 μM methylmannoside (B), a parameter that affords a means (eqn. 1d) of determining the equilibrium constant for the competing interaction of the second saccharide with immobilized lectin.

strength (I) I 0.5) [19]; and are also in reasonable agreement with literature reports [4,5] of 16 000–26 000 and 7 400–8 500 M^{-1} for the respective interactions of p-nitrophenylmannoside and methylmannoside with immobilized concanavalin A under fairly similar conditions (pH 5.5, I 0.1 and pH 6.0, I 0.5, respectively).

The next step of this experimental study of the competition between methylmannoside (B) and p-nitrophenylmannoside (A) for sites on immobilized concanavalin A is to entail analysis of the flow-rate dependence of the second moment of elution profiles for A in terms of k_{-1}^{obs}, an apparent first-order rate constant for dissociation of AX complex in the presence of a free concentration [B] of competing ligand. Lack of an analytical expression for the dependence of k_{-1}^{obs} upon the concentration of either saccharide has necessitated resort to numerical simulations of the chromatographic behaviour in order to ascertain the effect of the competing ligand (B) on the flow-rate dependence of the spread of A, which is interpreted as an apparent first-order rate constant (k_{-1}^{obs}) via eqn. 2. Further consideration of the experimental results is therefore preceded by a description of those simulations and of their outcome.

Simulated chromatographic migration of saccharide mixtures on immobilized concanavalin A

In anticipation of experimental studies of the effect of methylmannoside (B) on the affinity chromatographic behaviour of p-nitrophenylmannoside (A) on immobilized concanavalin A, elution profiles were simulated numerically for mixtures of A and B, whose interactions with immobilized-lectin sites (X) were described by eqns. 3a and 3b with k_{-1} = 0.42 s^{-1} (see later), $K_{AX} = k_{+1}/k_{-1} = 24\,000$ M^{-1}, $k_{-2} = 0.2$–2.0 s^{-1}, $K_{BX} = k_{+2}/k_{-2} = 10\,000$ M^{-1}. For generation of the trailing elution profile each segment (plate) of the column was assigned a total matrix-site concentration, $[\bar{\bar{X}}]$, of 32.5 μM (Fig. 1), the corresponding value for the competing ligand, $[\bar{B}]$, being set at 100 μM: the total concentration of partitioning solute, $[\bar{A}]$, was varied between 10 and 40 μM to define the effect of solute concentration upon the magnitude of k_{-1}^{obs} evaluated from the flow-rate dependence of σ_A^2 (eqn. 2). The trailing elution profile was then generated by successive introductions, to the top segment of the column array, of the transfer volume (δV) of solvent containing competing ligand B at its equilibrium concentration ([B]) in the array of segments at $t = 0$. For the advancing elution profile the starting condition was an array of segments with the concentrations of free matrix sites ([X]) and free competing ligand ([B]) set at the values required to establish a final plateau with the same total concentrations ($[\bar{\bar{X}}]$, $[\bar{A}]$ and $[\bar{B}]$) as those used for the initial conditions in simulation of the corresponding trailing elution profile.

The effects of column flow-rate upon the form of the elution profiles for solute ($[\bar{A}] = 40$ μM) in the presence of competing ligand ($[\bar{B}] = 100$ μM) are illustrated in Fig. 2: in this particular example $k_{-2} = 0.55$ s^{-1}. An obvious feature of these simulated elution profiles is the sharper form of the advancing boundary at the lower flow-rate, a situation consistent with chromatographic migration of a system exhibiting non-linear (Langmuir) kinetics [7]. A second point to note is that the extent of spreading of boundaries (advancing and trailing) increases with increasing flow rate, this being a manifestation of the comparable rates of chemical dissociation and chromatographic migration of the partitioning solute. Furthermore, the pronounced asymmetry of boundaries that is generated in these numerical simulations of chromatographic migration at higher flow-rates is also observed experimentally in affinity chromatography of p-nitrophenylmannoside–methylmannoside mixtures on immobilized concanavalin A (Fig. 3). Finally, the flow-rate dependence of the spread, as monitored by the second moment of the boundary (σ_A^2) was found to decrease with increasing concentration of solute.

The quantitative ramifications of that final point for the advancing elution profile are summarized in Fig. 4a, which presents the flow-rate dependence of the second moment derived from simulated advancing profiles for systems with 10–40 μM p-nitrophenylmannoside ($[\bar{A}]$). The consequent dependence of k_{-1}^{obs}, obtained from

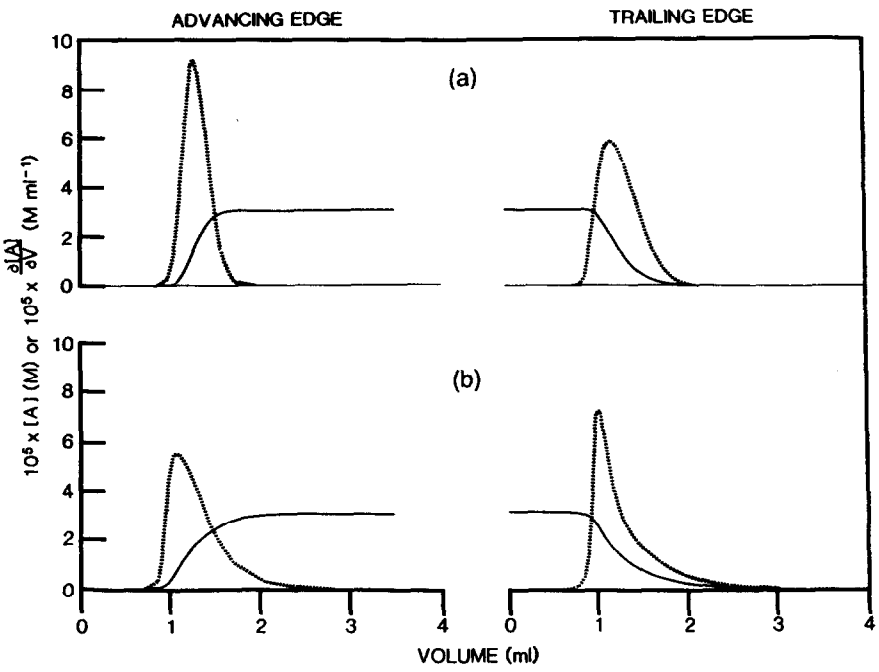

Fig. 2. Effect of flow-rate (F) on simulated elution profiles for the frontal chromatography of mixtures of p-nitrophenylmannoside (A) and methylmannoside (B) on an immobilized concanavalin A affinity column ($[\bar{X}] = 32.5\ \mu M$, $[\bar{A}] = 40\ \mu M$, $[\bar{B}] = 100\ \mu M$, $K_{AX} = 24\,000\ M^{-1}$, $k_{-1} = 0.42\ s^{-1}$, $k_{-2} = 0.55\ s^{-1}$): (a) $F = 1.0$ ml/min; (b) $F = 5.0$ ml/min. Solid lines denote the concentration profiles and broken lines the derivatives thereof.

Fig. 4a via eqn. 2, upon the concentration of free solute in the plateau region ([A]) is shown (○) in Fig. 4b. Also shown are corresponding dependences obtained for mixtures supplemented with 100 μM competing saccharide, the desorption of which from matrix sites is governed by an association equilibrium constant of 10 000 M^{-1} and dissociation rate constants of 0.2 (■) and 1.0 (▲) s^{-1}. Several points merit comment. (i) As noted previously [7], extrapolation of k_{-1}^{obs} to zero concentration in the absence of B essentially yields the value of k_{-1} (0.42 s^{-1}) that was used for the simulation of chromatographic migration. (ii) Fig. 4b also shows that the corresponding ordinate intercept is again essentially k_{-1} in situations where the interaction of partitioning solute with matrix sites is in competition with a matrix–ligand interaction. (iii) Although no information on the dissociation kinetics of competing ligand from the matrix emanates from the extrapolated value of k_{-1}^{obs} as $[A] \rightarrow 0$, the slope of the concentration dependence of k_{-1}^{obs} is a function of k_{-2} (Fig. 4b). Despite the absence of a quantitative expression for this concentration dependence, an empirical relationship may be obtained from simulated elution profiles for a range of assigned k_{-2} values. The resultant dependence, normalized by dividing by the slope of the absence of B, is presented in Fig. 5 to provide a standard curve for evaluating k_{-2} on the basis of the measured ratio of slopes, since the magnitudes of k_{-1}, K_{AX}, K_{BX} and $[\bar{X}]$ used in the simulations mimic the experimentally determined values for the interactions of p-nitrophenylmannoside and methylmannoside with immobilized concanavalin A. Such evaluation of k_{-2} is now illustrated by means of the experimental study of the effect of methylmannoside on the chromatographic behaviour of p-nitrophenylmannoside on the affinity column with concanavalin A as the immobilized ligand.

Rate constants for dissociation of saccharides from complexes with immobilized concanavalin A

The above numerical simulations refer to situations in which any partition of solute and

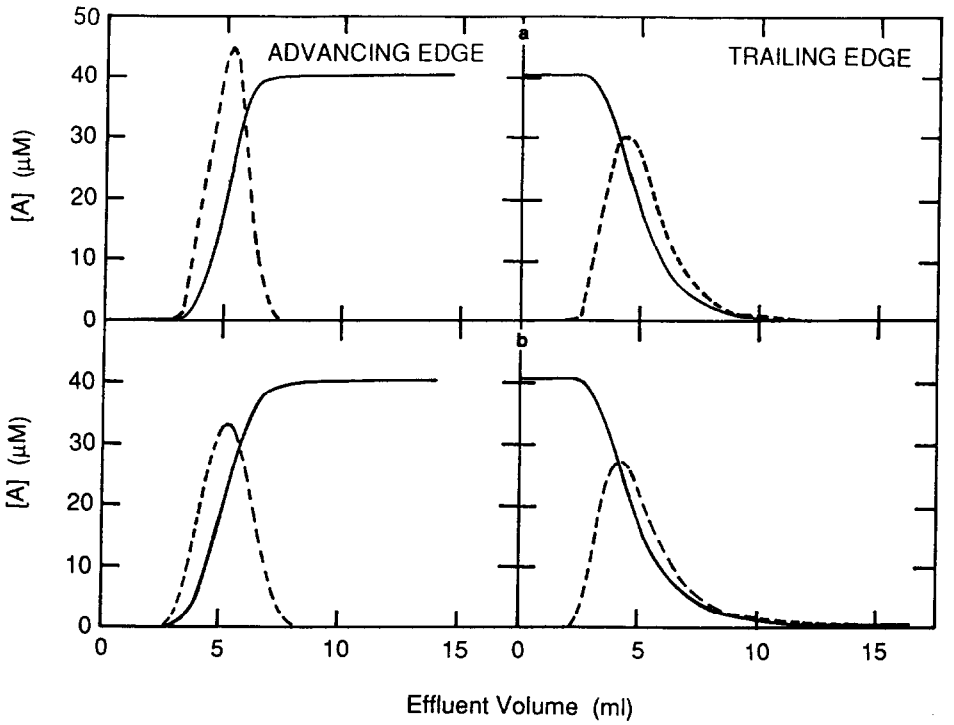

Fig. 3. Effect of flow-rate (F) on experimental elution profiles in affinity chromatography of mixtures of p-nitrophenylmannoside (A) and methylmannoside (B) in phosphate–chloride buffer (pH 5.5, I 0.5) on a column (25 × 0.46 cm) of glyceryl-CPG 3000 with concanavalin A as immobilized ligand ($[\bar{X}] = 32.5\ \mu M$, $[A] = 40\ \mu M$, $[B] = 100\ \mu M$): (a) $F = 2.2$ ml/min; (b) $F = 8.7$ ml/min. Solid lines denote the concentration profiles and broken lines the derivatives thereof.

competing ligand is identical and essentially instantaneous on the time scale of the dissociation kinetics. Our envisaged method of achieving conformity with this requirement entailed covalent attachment of concanavalin A to the surface of impenetrable glass beads, and hence confinement of both saccharides to the mobile phase of the column. However, the surface area needed for attainment of an acceptable concentration of immobilized lectin sites ($[\bar{X}]$) would have dictated the selection of beads with a diameter too small to be commensurate with the envisaged flow rates. Resort to the column of large porous glass beads (CPG 3000, 200 mesh) overcomes the surface-area problem but introduces the necessity of establishing the extent to which it is a reasonable approximation to assume that partition kinetics contributes negligibly to the flow-rate dependence of boundary spreading, $d\sigma_A^2/dF$.

Fig. 6 compares the flow-rate dependence of σ_A^2 obtained from advancing (○) and trailing (□) profiles for p-nitrophenylmannoside (40 μM) on the present lectin–CPG 3000 column with that obtained for either boundary on an identical column of underivatized CPG 3000 (▲). The slight positive slope of the latter plot indicates the existence of a non-negligible contribution by partition kinetics to the overall flow-rate dependence of boundary spreading. On the grounds that the coefficient describing the linear dependence of σ_A^2 upon flow-rate reflects the combined contributions of chemical, $(\sigma_A^2)_c$, and partition, $(\sigma_A^2)_p$, kinetics [22], effects of the latter have been taken into account by means of the expression

$$d(\sigma_A^2)_c/dF = d\sigma_A^2/dF - d(\sigma_A^2)_p/dF \quad (4)$$

which assumes simple additivity of the two contributions and introduces the problem of quantifying the partition kinetics contribution.

If chemical equilibrium between matrix sites and partitioning sites were instantaneous, all flow-rate dependence of the second moment would result from partition kinetics. Under those

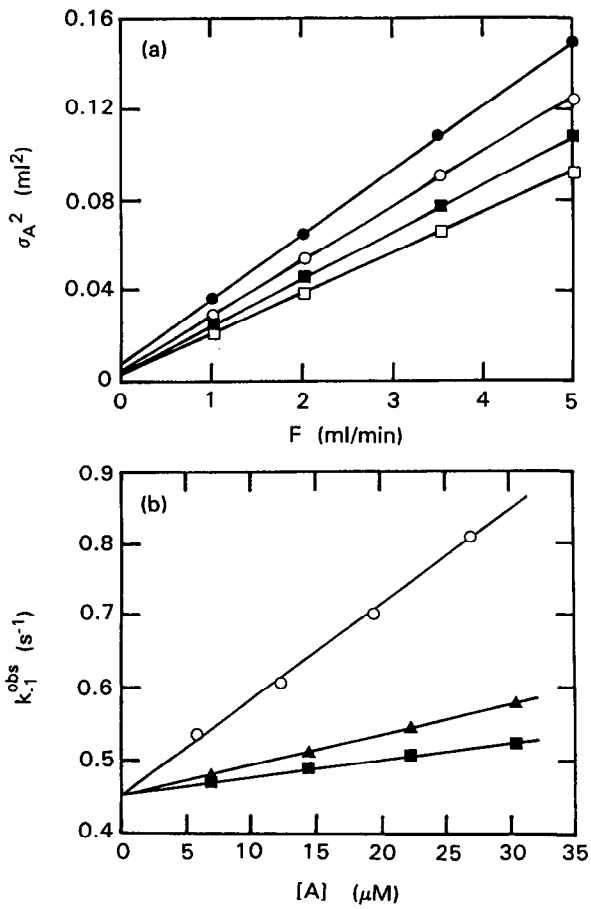

Fig. 4. Analysis of simulated elution profiles for the chromatography of *p*-nitrophenylmannoside on immobilized concanavalin A ($[\bar{X}] = 32.5\ \mu M$, as in Fig. 2). (a) Effect of flow-rate on the variance of advancing elution profiles with applied solute concentrations ([A]) of 5.9 (●), 12.5 (○), 19.6 (■) and 27.2 (□) μM saccharide. (b) Dependence of the apparent rate constant for *p*-nitrophenylmannoside desorption (○), obtained from eqn. 2, upon concentration of saccharide in the applied solution. Solid symbols denote corresponding dependences for mixtures supplemented with 86–89 μM competing saccharide ($[\bar{B}] = 100\ \mu M$), the desorption of which from matrix sites is governed by an equilibrium constant (K_{BX}) of 10 000 M^{-1} and dissociation rate constants (k_{-2}) of 0.2 (■) and 1.0 (▲) s^{-1}.

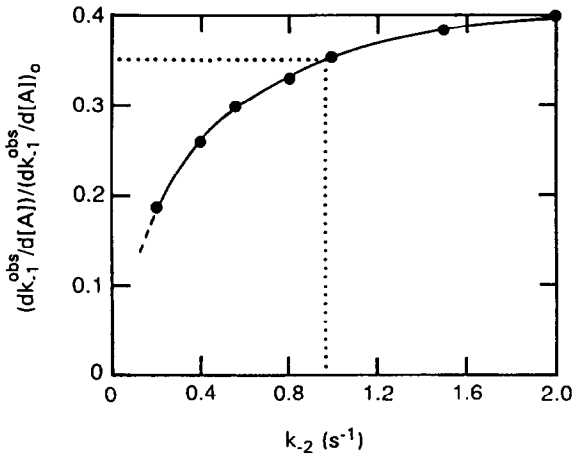

Fig. 5. Calibration plot, based on results of numerical simulations (Fig. 4), for evaluating k_{-2}, the rate constant for dissociation of methylmannoside from immobilized concanavalin A, from the effect of this competing saccharide (B) on the affinity chromatographic behaviour of *p*-nitrophenylmannoside (A). The ordinate presents the concentration dependence of the apparent rate constant for dissociation of the AX complex in the presence of competing saccharide ($[\bar{B}] = 100\ \mu M$), $(dk_{-1}^{obs}/d[A])$, as a proportion of the corresponding slope in the absence of competing saccharide, $(dk_{-1}^{obs}/d[A])_0$. Dotted lines indicate the magnitude of the experimentally determined ratio (Fig. 7) and the consequent estimate of k_{-2}.

circumstances the elution volume, $\bar{V}_A$, and second moment, $(\sigma_A^2)_p$, are given by [16]

$$\bar{V}_A = \{1 + K_p(1 + K_{AX}[X])\}V_0 \quad (5a)$$

$$(\sigma_A^2)_p = \{2K_p(1 + K_{AX}[X])^2/k_{-p}\}V_0F \quad (5b)$$

where K_p is the partition coefficient for equilibrium attainment between the mobile phase (with volume V_0) and the accessible stationary phase volume (with volume $V_A^* - V_0$): k_{-p} refers to the rate constant for the partitioning process. Experimentally more tractable relationships are obtained on noting [7] that

$$K_{AX}[X] = (\bar{V}_A - V_A^*)/V_A^* \quad (6)$$

whereupon eqns. 5a and 5b become

$$\bar{V}_A = [1 + K_p(\bar{V}_A/V_A^*)]V_0 \quad (7a)$$

$$(\sigma_A^2)_p = 2K_p(\bar{V}_A/V_A^*)^2V_0F/k_{-p} \quad (7b)$$

Combination of eqns. 7a and 7b then gives

$$d(\sigma_A^2)_p/dF = 2(\bar{V}_A - V_0)(\bar{V}_A/V_A^*)/k_{-p} \quad (8)$$

The experimentally measured flow-rate dependence of the second moment reflecting partition

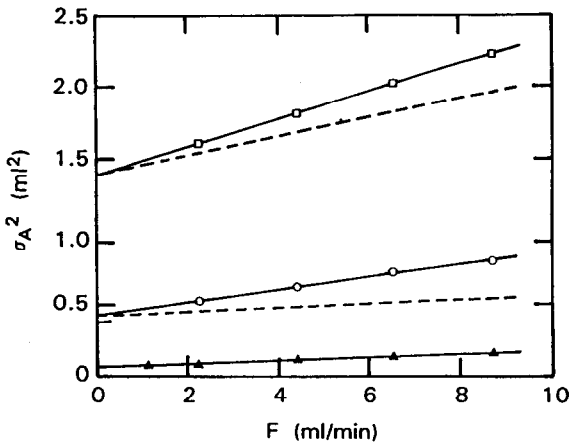

Fig. 6. Effect of flow-rate on the second moment of the advancing (○) and trailing (□) elution profiles of *p*-nitrophenylmannoside (40 μM) on an affinity column (25 × 0.46 cm) of glyceryl-CPG 3000 with concanavalin A as the immobilized ligand. Broken lines denote the corresponding dependences after allowance for effects of flow-rate on boundary spreading arising from the kinetics of saccharide partitioning into the stationary phase, a correction made by applying eqns. 4 and 10 to results (▲) obtained from advancing and trailing elution profiles in chromatography of *p*-nitrophenylmannoside on an identical column of underivatized glyceryl-CPG 3000: V_0 was taken as 2.00 ml for this column with a bed volume of 4.15 ml [20,21].

kinetics on the underivatized column (▲, Fig. 6) is now incorporated by noting that the analog of eqn. 8 for that experiment is, by the above reasoning but with $[X] = 0$ and $\bar{V}_A = V_A^*$,

$$d(\sigma_A^2)_{p,u}/dF = 2(V_A^* - V_0)/k_{-p} \quad (9)$$

Elimination of k_{-p} between eqns. 8 and 9 then gives

$$d(\sigma_A^2)_p/dF = \frac{\bar{V}_A(\bar{V}_A - V_0)[d(\sigma_A^2)_{p,u}/dF]}{V_A^*(V_A^* - V_0)} \quad (10)$$

as the term to be subtracted from the measured value of $d\sigma_A^2/dF$ in an affinity chromatographic experiment in order to obtain the chemical kinetic contribution (eqn. 4).

The consequent flow-rate dependence of $(\sigma_A^2)_c$ for *p*-nitrophenylmannoside in the absence of B is shown as the broken lines in Fig. 6, the slopes of which may be used to evaluate the magnitudes of k_{-1}^{obs}, via eqn. 2. As noted above, such values need to be extrapolated to zero solute concentration in order to obtain k_{-1}, the rate constant for dissociation of the AX complex. Such dependence of k_{-1}^{obs} upon concentration of *p*-nitrophenylmannoside in the applied solution is shown (open symbols) in Fig. 7, which also presents the corresponding relationships deduced from experiments with mixtures containing 100 μM methylmannoside (closed symbols): squares and circles refer to the respective results inferred from advancing and trailing elution profiles. On the basis of the ordinate intercept for experiments in the absence of B a value of 0.42 s^{-1} is obtained for k_{-1}, the rate constant for dissociation of *p*-nitrophenylmannoside from its complex with immobilized concanavalin A. In that regard the slightly higher value of the corresponding intercept in the presence of methylmannoside is at variance with the earlier inference, drawn from the results of the numerical simulations (Fig. 4b), that this extrapolation should also yield k_{-1}; and possibly reflects the presence of a minor systematic error in the analysis due to assumed simple additivity of partition- and chemical-kinetic contributions to the flow-rate

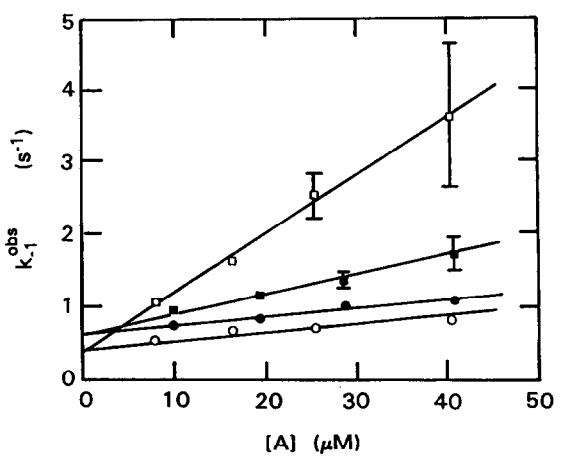

Fig. 7. Effect of methylmannoside (100 μM) on the magnitude of the apparent rate constant for desorption of *p*-nitrophenylmannoside (A) from immobilized concanavalin A, a parameter obtained (eqn. 2) from the flow-rate dependence of boundary spreading (Fig. 4): □, ○ = respective values of k_{-1}^{obs} obtained from advancing and trailing elution profiles for A in the absence of competing saccharide; ■, ● = corresponding values obtained from experiments on mixtures supplemented with 100 μM methylmannoside.

dependence of boundary spreading. Interpretation of the slope of the dependence of $(\sigma_A^2)_c$ upon [A] that is obtained from the advancing elution profile in the presence of 100 μM methylmannoside in terms of the calibration plot (Fig. 5) leads to a value of 0.9–1.1 s^{-1} for k_{-2}, the rate constant for dissociation of the complex between immobilized concanavalin A and methylmannoside (the competing ligand, B). In principle, this value is likely to be a slight underestimate because the calibration plot refers to mixtures with slightly lower concentrations of competing saccharide (86–89 μM *cf.* 100 μM in the experiments). However, the scatter of experimental points in the dependence of k_{-1}^{obs} upon [A] (Fig. 7) is sufficiently great to encompass the ensuing error. We therefore assign k_{-2} a value of 1 s^{-1} on the basis of these experiments.

To conclude this experimental section on characterizing the kinetics of interactions between saccharides and immobilized concanavalin A, we note that the present rate constant of 0.42 s^{-1} for the dissociation of *p*-nitrophenylmannoside agrees well with a corresponding estimate of 0.37–0.43 s^{-1} that is obtained by extrapolating zonal chromatographic results to zero for the concentration of the injected zone (Table III in ref. 4). In addition, the larger rate constant (k_{-2}) of 1 s^{-1} that is inferred from Figs. 5–7 for dissociation of methylmannoside from immobilized concanavalin A is in keeping with the smaller binding constant (10 000 *cf.* 24 000 M^{-1}) that pertains to this competitive interaction. These results point to the potential of employing a calibration plot based on results of numerical simulations of affinity chromatographic behaviour for evaluating the kinetics of the second interaction in instances where ligand-facilitated elution of the partitioning solute (A) reflects competition from the ligand (B) for affinity matrix sites (X). Finally, the fact that these rate constants are smaller, by an order of magnitude, than those for the corresponding saccharide interactions with soluble concanavalin A [8] should not be construed as a deficiency of the affinity chromatographic analysis but rather as a consequence of the chemical modification associated with lectin immobilization.

Simulated migration of ligand-facilitated elution reflecting competitive binding of ligand to solute

Thus far the emphasis of this investigation has centred on the feasibility of evaluating rate constants for the competitive interaction in affinity chromatographic situations where the ligand-facilitated elution of solute (A) reflects competition with ligand (B) for matrix sites (X). We conclude this investigation by employing simulated chromatographic migration to explore the alternative situation in which the ligand-facilitated elution reflects an interaction in the liquid phase between solute (A) and ligand (B). The simulated results could be considered to describe, for example, affinity chromatography of mixtures of a lectin and *p*-nitrophenylmannoside on immobilized concanavalin A, or of mixtures of NAD^+ (A) and alcohol dehydrogenase (B) on an affinity matrix with the enzyme as immobilized ligand [3]. In that regard the magnitudes of the equilibrium and rate constants for the dissociation of AX and AB complexes have been amended to be more in line with those for the latter system at alkaline pH [23,24] to illustrate the feasibility of quantifying the kinetics of reactions in instances where the dissociation rate constants are greater than those already considered.

The potential of affinity chromatography for evaluating the dissociation rate constant for a competing interaction between ligand and solute in the liquid phase has been explored by numerical simulation of trailing elution profiles for systems with $[\bar{X}] = 5\ \mu M$, $[\bar{B}] = 4\ \mu M$, $K_{AX} = 10^5\ M^{-1}$ and $k_{-1} = 4\ s^{-1}$. For initial simulations the equilibrium constant (K_{AB}) and rate constant for dissociation constant of the solute-ligand complex in solution (k_{-3} in eqn. 3c) were also taken as $10^5\ M^{-1}$ and 4 s^{-1}, respectively. However, for exploration of a wider range of potential systems, k_{-3} was decreased and $K_{AB} = k_{+3}/k_{-3}$ increased accordingly such that the other extreme situation reflected a system with $k_{-3} = 0.4\ s^{-1}$ and $K_{AB} = 10^6\ M^{-1}$. To avoid the problems of differential migration of A, B and AB in the liquid phase, the column (20×0.46 cm) was again considered to contain X-sites immobilized to an impenetrable matrix, whereupon V_A^*

becomes synonymous with the void volume of the column.

In comparison with the treatment of their counterparts described above, the quantification of these systems with the competitive interaction between ligand and solute is rendered far more elegant by the availability of the following expression [16]

$$(d\sigma_A^2/dF) = \frac{2V_A^* K_{AX}[X]}{1 + K_{AB}[B]} \cdot \left\{ \frac{1}{k_{-1}} + \frac{K_{AB}K_{AX}[X][B]}{k_{-3}(1 + K_{AB}[B])^2} \right\} \quad (11)$$

which describes the flow-rate dependence of boundary spreading under conditions of linear kinetics. After substituting eqn. 6 for $K_{AX}[X]$, eqn. 11 becomes

$$(d\sigma_A^2/dF) = \frac{2(\bar{V}_A - V_A^*)}{(1 + K_{AB}[B])} \cdot \left\{ \frac{1}{k_{-1}} + \frac{K_{AB}(\bar{V}_A - V_A^*)[B]}{k_{-3}V_A^*(1 + K_{AB}[B])^2} \right\} \quad (12)$$

which, as required, simplifies to eqn. 2 in the absence of competing ligand ([B] = 0). The approach to be adopted therefore entails substitution of the value of k_{-1}, obtainable experimentally from data in the absence of B (Figs. 4 and 6), the two measured elution volumes ($\bar{V}_A$, V_A^*) and equilibrium constants (K_{AX}, K_{AB} [12–14]) into eqn. 12 to obtain an apparent estimate of the rate constant for dissociation of AB complex, k_{-3}^{obs}, from the flow-rate dependence of boundary spreading in a series of experiments with given free concentrations of solute and ligand ([A] and [B], respectively). Because eqn. 12 has been derived on the basis of linear kinetics [16], the true value of k_{-3} should then be given by the limiting value of k_{-3}^{obs} as [A] → 0. A series of such experiments on mixtures with a range of concentrations of solute, [Ā], is then required for this extrapolation to infinite dilution.

Results of simulations with values of 4.0 s^{-1} (●) and 0.4 s^{-1} (▲) for k_{-3} and a range of total solute concentrations are summarized in Fig. 8,

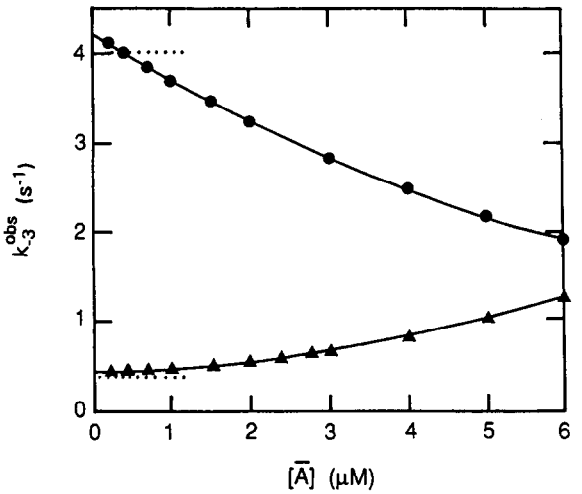

Fig. 8. Analysis of simulated trailing elution profiles, in accordance with eqn. 12, to test the feasibility of employing flow-rate dependence of boundary spreading in affinity chromatography of a solute (A) to evaluate the dissociation rate constant (k_{-3}) for a competing reaction between solute and ligand (B) in the liquid phase. Points refer to results from simulated elution profiles for a system with $[\bar{X}] = 5\ \mu M$, $[\bar{B}] = 4\ \mu M$, $K_{AX} = 10^5\ M^{-1}$, $k_{-1} = 4\ s^{-1}$ and either $K_{AB} = 10^5\ M^{-1}$, $k_{-3} = 4\ s^{-1}$ (●) or $K_{AB} = 10^6\ M^{-1}$, $k_{-3} = 0.4\ s^{-1}$ (▲). Dotted lines denote the input values of k_{-3} that should, in principle, be obtained from eqn. 12 in the limit that the concentration of *p*-nitrophenylmannoside tends to zero.

about which the following points are noted. (i) Values of k_{-3}^{obs} for these two situations signify that their required extrapolation to zero solute concentration to obtain k_{-3} should pose no great difficulty, despite the fact that the form of the extrapolation is clearly a function of the magnitude of k_{-3} (or, more generally a function of the magnitude of k_{-3} relative to that of k_{+3}). (ii) Extrapolation of the two sets of the k_{-3}^{obs} data to infinite dilution yields estimates of 4.2 and 0.44 s^{-1} for the respective dissociation rate constants (k_{-3}). (iii) Such ability to regain the input values to within 10% is considered to be sufficiently satisfactory to justify an optimistic outlook to the prospect of using affinity chromatography for quantifying the kinetics of complex dissociation (and hence complex formation via K_{AB}) in the solution phase. (iv) This finding is particularly encouraging in the sense that the major envisaged deployment of affinity chromatography entails the characterization of a competitive

interaction between solute and ligand in the liquid phase. In other words, the affinity matrix is likely to be introduced merely as a tool for characterizing the kinetics of an equilibrium interaction that occurs in the solution phase.

CONCLUDING REMARKS

This investigation culminates a probe of the possibility that affinity chromatography might provide a means of obtaining dissociation rate constants for reactions that are too slow for study by stopped-flow techniques. In that regard, the optimistic conclusion to this study contrasts markedly with the disappointing outcomes of its predecessors [1–6], and also the criticism [25] of the whole approach. As noted previously [7], a major contributing factor to the greatly improved outlook for affinity chromatography as a means of studying the dissociation kinetics of reactions has been the replacement of zonal by frontal affinity chromatography in order to avoid the theoretical requirement that two infinitely sharp boundaries be generated an infinitesimal distance apart. Another change in approach has been the quantification of the kinetic contribution to boundary spreading on the basis of the flow-rate dependence of the second moment, thereby obviating the problem of making allowance for the contribution arising from axial dispersion [3–5]. Advantage has also been taken of the fact that frontal chromatography defines unequivocally the solute concentration to which chromatographic parameters refer, and that results obtained under conditions of non-linear (Langmuir) kinetics may therefore be extrapolated to zero solute concentration for analysis in terms of the simpler quantitative expressions describing chromatographic migration under linear kinetic conditions. However, despite the considerable progress that has been made in the characterization of reaction kinetics by affinity chromatography, it should be noted that univalency of the solute is an implicit assumption in the above simulations and experimental studies. Indeed, this consideration has dictated the need to design the experiments (simulated or otherwise) in such a manner that the protein (concanavalin A or alcohol dehydrogenase) rather than the small solute (saccharide or pyridine nucleotide) is attached to the chromatographic matrix: the procedures described are not applicable to the reverse situation entailing affinity chromatography of the proteins with the small solute immobilized to a matrix.

The present investigation also serves to exemplify even further the power of numerical simulation as an aid to the development of quantitative procedures for characterizing interactions on the basis of their effects on chromatographic migration [7,26,27]. For example, simulation of the affinity chromatographic behaviour of a solute in the presence of a ligand with which it also interacts has afforded the means of establishing the validity of defining the competing dissociation rate constant (k_{-3}) on the basis of expressions developed by Hethcote and DeLisi [16] for diffusion-free migration under linear kinetic conditions (Fig. 8). Even greater testimony to the power of numerical simulation emanates from consideration of the affinity chromatography of systems in which solute and ligand compete for matrix sites, a situation for which no quantitative description of boundary spreading is available. Despite the consequent lack of an analytical expression for description of results, it has still been possible to evaluate a rate constant for the dissociation of methylmannoside from immobilized concanavalin A on the basis of the effect of this competing ligand on the affinity chromatographic behaviour of *p*-nitrophenylmannoside on a column of porous glass beads with the lectin covalently attached (Figs. 5–7).

Finally, it should be noted that the ramifications of this particular investigation extend beyond the feasibility of employing affinity chromatography to quantify the kinetics of equilibrium interactions that are amenable to study by stopped-flow and temperature-jump techniques: indeed, their readier study by the latter methods is not disputed. This demonstration of the viability of affinity chromatography for characterizing the kinetics of reactions occurring on that time scale means that the procedure may also be used to quantify the kinetics of any slower interaction merely by decreasing the range of column flow-rates used to assess the effect of

chemical kinetics on the extent of boundary spreading. The most important outcome of this investigation is therefore the development of a protocol whereby affinity chromatography affords a means of characterizing the dissociation kinetics of interactions that are too slow for study by stopped-flow methods but too fast for study by assaying the time dependence of product formation (or reactant depletion) — a long-sought potential [1–6] of affinity chromatography that is at last being realized.

ACKNOWLEDGEMENTS

The support of this investigation by the Australian Research Council (D.J.W.) and the University of Colorado Cancer Center (J.R.C.) is gratefully acknowledged, as is the excellent technical assistance of Robert O. Coombs in the numerical simulation aspects of this work.

REFERENCES

1 I.M. Chaiken, *Anal. Biochem.*, 97 (1979) 1.
2 V. Kasche, K. Bucholz and B. Galunsky, *J. Chromatogr.*, 216 (1981) 169.
3 K. Nilsson and P.-O. Larsson, *Anal. Biochem.*, 134 (1983) 72.
4 A.J. Muller and P.W. Carr, *J. Chromatogr.*, 284 (1984) 33.
5 D.J. Anderson and R.R. Walters, *J. Chromatogr.*, 376 (1986) 69.
6 R.R. Walters, in I.M. Chaiken (Editor), *Analytical Affinity Chromatography*, CRC Press, Boca Raton, FL, 1987, p. 117.
7 D.J. Winzor, P.D. Munro and J.R. Cann, *Anal. Biochem.*, 194 (1991) 54.
8 S.D. Lewis, J.A. Schafer and I.J. Goldstein, *Arch. Biochem. Biophys.*, 172 (1976) 689.
9 F.G. Loontiens, R.M. Clegg, A. Van Landschoot and T.M. Jovin, *Eur. J. Biochem.*, 78 (1977) 465.
10 P.J. Hogg and C.M. Jackson, *Proc. Natl. Acad. Sci. U.S.A.*, 86 (1989) 3619.
11 D.J. Winzor, *J. Chromatogr.*, 597 (1992) 67.
12 L.W. Nichol, L.D. Ward and D.J. Winzor, *Biochemistry*, 20 (1981) 4856.
13 P.J. Hogg and D.J. Winzor, *Arch. Biochem. Biophys.*, 234 (1984) 55.
14 P.J. Hogg and D.J. Winzor, *Biochim. Biophys. Acta*, 843 (1985) 159.
15 H.W. Hethcote and C. DeLisi, *J. Chromatogr.*, 240 (1982) 269.
16 H.W. Hethcote and C. DeLisi, *J. Chromatogr.*, 248 (1982) 183.
17 E. Gleuckauf, *Trans. Faraday Soc.*, 51 (1955) 34.
18 S.W. Benson, *The Foundations of Chemical Kinetics*, McGraw-Hill, New York, 1960, p. 29.
19 D.J. Winzor, P.D. Munro and C.M. Jackson, *J. Chromatogr.*, 597 (1992) 57.
20 L.W. Nichol, R.J. Siezen and D.J. Winzor, *Biophys. Chem.*, 10 (1979) 17.
21 R.J. Siezen, L.W. Nichol and D.J. Winzor, *Biophys. Chem.*, 14 (1981) 221.
22 E.D. Katz, K.L. Ogan and R.P.W. Scott, *J. Chromatogr.*, 270 (1983) 51.
23 H. Theorell, A.P. Nygaard and R. Bonnichsen, *Acta Chem. Scand.*, 9 (1955) 1148.
24 H. Theorell and J.S. McKinley-McKee, *Acta Chem. Scand.*, 15 (1961) 1797.
25 G.H. Weiss, *Sep. Sci. Technol.*, 16 (1981) 75.
26 J.R. Cann and D.J. Winzor, *Arch. Biochem. Biophys.*, 256 (1987) 78.
27 J.R. Cann, A.G. Appu Rao and D.J. Winzor, *Arch. Biochem. Biophys.*, 270 (1989) 173.